

*Property 1:* Let  $a \in \mathcal{P}^n$  and separate  $a$  into its even and odd parts,  $a_e$  and  $a_o$ ,

$$a(s) = a_e + a_o = a_e(s^2) + s\bar{a}_o(s^2) \quad (35)$$

where the notation  $a_e(s^2)$  and  $\bar{a}_o(s^2)$  is used to enhance the fact that  $a_e$  and  $\bar{a}_o$  contain only even powers. Then,  $a$  is Hurwitz if and only if there exists  $\lambda_i$ ,  $\xi_j$ , and  $c \in \mathcal{R}$  satisfying

$$a_e(-\omega^2) = (\lambda_1 - \omega^2)(\lambda_2 - \omega^2) \cdots (\lambda_{n/2} - \omega^2) \quad (36)$$

$$\bar{a}_o(-\omega^2) = c(\xi_1 - \omega^2)(\xi_2 - \omega^2) \cdots (\xi_{n/2-1} - \omega^2) \quad (37)$$

where  $c > 0$  and  $0 < \lambda_1 < \xi_1 < \lambda_2 < \xi_2 < \cdots < \lambda_{n/2}$ .

*Lemma 1:* Consider a Hurwitz polynomial  $q$  and let  $q_e$  and  $q_o$  denote its even and odd parts. Then there exists an even function  $u$  and an odd function  $v$  satisfying

$$q_e(s)u(s) + q_o(s)v(s) = 1. \quad (38)$$

*Proof:* Equation (38) is a Bezout identity and its satisfaction is equivalent to the statement that  $q_e(s)$  and  $q_o(s)$  are coprime. To show this, we reason by contradiction. Suppose  $q_e$  and  $q_o$  are not coprime. In this case we must have,

$$q_e(s) = a(s)f(s) \quad (39)$$

$$q_o(s) = b(s)f(s) \quad (40)$$

for some nontrivial polynomial  $f(s)$ . In this case, one of the following must be true,

$$f \text{ even} \Rightarrow a \text{ even and } b \text{ odd} \quad (41)$$

$$f \text{ odd} \Rightarrow a \text{ odd and } b \text{ even.} \quad (42)$$

We assume without loss of generality that (41) holds and  $q$  is even. In this case,  $q_e$  and  $q_o$  can be rewritten as follows,

$$\begin{aligned} q_e(s^2) &= a(s^2)f(s^2) = (a_1 + a_2s^2 + a_4s^4 + \cdots) \\ &\quad \times (f_0 + f_2s^2 + f_4s^4 + \cdots) \\ q_o(s^2) &= s\bar{b}(s^2)f(s^2) = s(b_1 + b_3s^2 + b_5s^4 + \cdots) \\ &\quad \times (f_0 + f_2s^2 + f_4s^4 + \cdots) = s\bar{q}_o(s^2). \end{aligned}$$

Thus, if  $\{\zeta_1, \zeta_2, \dots, \zeta_m\}$  are the roots of  $f(-\omega^2)$ , we have

$$\begin{aligned} q_e(-\omega^2) &= a(-\omega^2)(\zeta_1 - \omega^2)(\zeta_2 - \omega^2) \cdots (\zeta_m - \omega^2) \\ \bar{q}_o(-\omega^2) &= b(-\omega^2)(\zeta_1 - \omega^2)(\zeta_2 - \omega^2) \cdots (\zeta_m - \omega^2). \end{aligned}$$

It follows that  $q$  is not Hurwitz, since the  $m$  roots of  $q_e(-\omega^2)$  and  $\bar{q}_o(-\omega^2)$  contained in  $f(-\omega^2)$  do not satisfy Property 1. This contradicts the assumptions. To complete the proof of Lemma 1 there remains to show that  $u$  and  $v$  are respectively even and odd. This is a straightforward consequence of the Euclidean algorithm (see, for example, [14]), by which  $u$  and  $v$  can be determined, and the even property of  $mu + nv = 1$ .  $\square$

#### REFERENCES

- [1] C. A. Desoer and M. Vidyasagar, *Feedback Systems: Input-Output Properties*. New York: Academic, 1975.
- [2] J. H. Taylor, "Strictly positive-real functions and the Lefschetz-Kalman-Yakubovich (LKY) lemma," *IEEE Trans. Circuits Syst.*, pp. 310-311, Mar. 1974.
- [3] P. Ioannou and G. Tao, "Frequency domain conditions for strictly positive real functions," *IEEE Trans. Automat. Contr.*, vol. 32, pp. 53-54, Jan. 1987.
- [4] H. J. Marquez and C. J. Damaren, "Comments on 'Strictly Positive Real Transfer Functions Revisited,'" submitted for publication.

- [5] K. J. Astrom and B. Wittenmark, *Adaptive Control*. Reading, MA: Addison-Wesley, 1989.
- [6] R. J. Benhabib, R. P. Iwens, and R. L. Jackson, "Stability of large space structure control systems using positivity concepts," *J. Guidance and Control*, vol. 4, pp. 487-494, Sept.-Oct. 1981.
- [7] C. A. Desoer, R. W. Liu, J. M. Murray, R. Saeks, "Feedback system design: The fractional representation approach to analysis and synthesis," *IEEE Trans. Automat. Contr.*, vol. 25, pp. 399-412, June 1980.
- [8] E. A. Guillemin, *Synthesis of Passive Networks*. New York: Wiley, 1957.
- [9] M. E. Van Valkenburg, *Introduction to Modern Network Synthesis*. New York: Wiley, 1960.
- [10] E. I. Jury, *Inners and Stability of Dynamic Systems*. New York: Wiley, 1974.
- [11] S. Lefschetz, *Stability of Nonlinear Control Systems*. New York: Academic, 1963.
- [12] J. C. Willems, "Dissipative dynamical systems, Part II: Linear systems with quadratic supply rates," *Arch. Rational Mech. Anal.*, vol. 45, pp. 352-393, 1972.
- [13] F. Gantmacher, *The Theory of Matrices*. New York: Chelsea, 1959, vol. II.
- [14] J. Gilbert and L. Gilbert, *Elements of Modern Algebra*. Boston, MA: PWS-Kent, 1992, third ed.

## On the Advantages of the LMS Spectrum Analyzer Over Nonadaptive Implementations of the Sliding-DFT

Françoise Beaufays and Bernard Widrow

**Abstract**—Based on the least mean squares (LMS) algorithm, the LMS spectrum analyzer can be used to recursively calculate the discrete Fourier transform (DFT) of a sliding window of data. In this paper, we compare the LMS spectrum analyzer with the straightforward nonadaptive implementation of the recursive DFT. In particular, we demonstrate the robustness of the LMS spectrum analyzer to the propagation of roundoff errors, a property that is not shared by other recursive DFT algorithms.

### I. INTRODUCTION

In some signal processing applications, a discrete time signal must be continuously analyzed in the frequency domain. At each instant, the  $N$  most recent samples of the input sequence are transformed by an  $N$ -point DFT. As a new data sample becomes available, the input window is shifted by one position forward in time, and a new DFT is evaluated. This is sometimes referred to as the *sliding-DFT* [1]. To save computations, the new DFT can be calculated recursively from the previous one. However, the propagation and accumulation of noise due for example to roundoff errors in floating point arithmetic makes it necessary to often reset the DFT. This increases the overall number of computations and adds to the complexity of the circuitry.

The *LMS spectrum analyzer* [2] can also perform the recursive computation of a sliding-DFT but because it relies on an adaptive

Manuscript received January 10, 1994; revised December, 6, 1994. This work was sponsored by EPRI under Contract RP8010-13 and by NSF under Grant NSF IRI 91-12531. This paper was recommended by Associate Editor Y. Inouye.

The authors are with the Department of Electrical Engineering, Stanford University, Stanford, CA 94305 USA.  
IEEE Log Number 9410008.

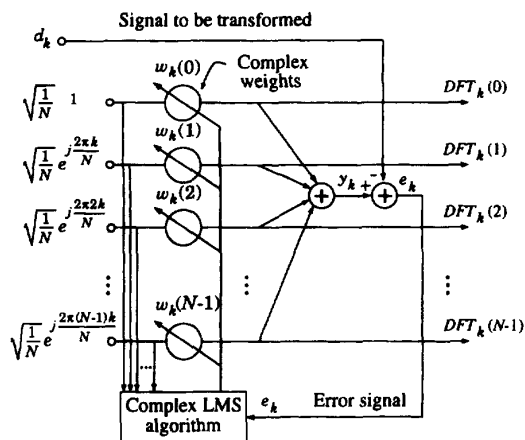


Fig. 1. The LMS spectrum analyzer.

technique, it automatically adjusts for possible errors. We show that actually *any* error appearing in the DFT is attenuated as it propagates over time, and is *completely eliminated* after a number of iterations equal to the length of the DFT.

## II. THE LMS SPECTRUM ANALYZER

The LMS spectrum analyzer is represented in Fig. 1. The signal to be Fourier transformed is used as the desired output  $d_k$  of a linear adaptive filter. The input to the filter at time  $k$  is the complex phasor

$$\mathbf{X}_k = \sqrt{\frac{1}{N}} \left[ 1 \quad e^{j\frac{2\pi k}{N}} \quad e^{j\frac{2\pi 2k}{N}} \quad \dots \quad e^{j\frac{2\pi(N-1)k}{N}} \right]^T, \quad (1)$$

where  $T$  denotes the transpose. The series of phasors  $\mathbf{X}_0, \mathbf{X}_1, \dots, \mathbf{X}_{N-1}, \mathbf{X}_N, \dots$  satisfies two important properties: first the series is periodic with period  $N$ , second  $\{\mathbf{X}_0, \mathbf{X}_1, \dots, \mathbf{X}_{N-1}\}$  form an orthonormal basis in the  $N$ -dimensional space.

The filter weight vector  $\mathbf{W}_k$  is adapted with the complex LMS algorithm [3]

$$\mathbf{W}_{k+1} = \mathbf{W}_k + 2\mu e_k \bar{\mathbf{X}}_k, \quad (2)$$

where  $\mu$  is the learning rate,  $\bar{\mathbf{X}}_k$  is the complex conjugate of  $\mathbf{X}_k$ , and  $e_k$  is the error signal defined as  $e_k = d_k - \mathbf{X}_k^T \mathbf{W}_k$ . Widrow *et al.* showed [2] that by setting the learning rate to  $1/2$ , by iterating over  $k$  from the initial conditions  $\mathbf{W}_0 = 0$ , and by using the above-mentioned properties of the input phasors, one finds for the weight vector

$$\mathbf{W}_k = \sum_{m=k-N}^{k-1} d_m \bar{\mathbf{X}}_m. \quad (3)$$

With the same notation, the DFT of the data samples  $d_{k-N}, \dots, d_{k-1}$ , can be expressed as

$$\text{DFT}_k = \sum_{m=k-N}^{k-1} d_m \bar{\mathbf{X}}_{m-k}. \quad (4)$$

The phasor  $\mathbf{X}_{m-k}$  is related to  $\mathbf{X}_m$  by the formula  $\mathbf{X}_{m-k} = \mathbf{P}^{-k} \mathbf{X}_m$ , where the diagonal matrix  $\mathbf{P}$  is defined as  $\mathbf{P} \triangleq \text{diag}\{1, e^{j2\pi/N}, e^{j2\pi 2/N}, \dots, e^{j2\pi(N-1)/N}\}$ . Comparing (3) and (4), one finds

$$\text{DFT}_k = \sum_{m=k-N}^{k-1} d_m \bar{\mathbf{X}}_{m-k} = \mathbf{P}^k \sum_{m=k-N}^{k-1} d_m \bar{\mathbf{X}}_m = \mathbf{P}^k \mathbf{W}_k. \quad (5)$$

At each instant  $k$ , the weight vector of the LMS filter is proportional to the DFT of the past  $N$  data samples.

It should be noted that the behavior of the LMS algorithm in the LMS spectrum analyzer is somewhat "special" in the sense that the LMS filter does not converge asymptotically and with misadjustment noise to its optimal solution as it usually does. Rather, it provides at each iteration the *exact* desired solution.

## III. NONADAPTIVE RECURSIVE IMPLEMENTATIONS OF THE DFT

By iteratively updating  $\mathbf{W}_k$ , the LMS spectrum analyzer evaluates the sliding-DFT recursively. A more straightforward but nonadaptive recursive implementation of the sliding-DFT [4] can be obtained by comparing the DFT at times  $k$  and  $k+1$  and by observing that

$$\begin{aligned} \text{DFT}_{k+1} &= \mathbf{P}^{k+1} \sum_{m=k+1-N}^k d_m \bar{\mathbf{X}}_m \\ &= \mathbf{P} \left( \text{DFT}_k + (d_k - d_{k-N}) \bar{\mathbf{X}}_0 \right). \end{aligned} \quad (6)$$

The operations performed by the LMS spectrum analyzer are very similar. The weight vectors at times  $k$  and  $k+1$  (see (3)) can be related by the formula

$$\mathbf{W}_{k+1} = \mathbf{W}_k + (d_k - d_{k-N}) \bar{\mathbf{X}}_0, \quad (7)$$

which is identical to (6) since the DFT and the weight vector at time  $k$  differ only by a multiplicative factor  $\mathbf{P}^k$  (5). Although the nonadaptive sliding-DFT and the LMS spectrum analyzer perform very similar operations, their behaviors in limited precision arithmetic differ drastically.

## IV. PROPAGATION OF ROUND-OFF ERRORS IN THE SLIDING-DFT

In software and hardware implementations, limited precision causes roundoff errors that propagate from iteration to iteration. In the sliding-DFT, since the elements of the multiplicative diagonal matrix  $\mathbf{P}$  in (6) all have modulus one, roundoff errors propagate unattenuated and accumulate over time. The LMS spectrum analyzer, on the contrary, has a "built-in" error cancellation mechanism.

Consider a situation where the weight vector of the LMS filter is free from errors up to time  $k-1$ . At time  $k$ , a noise vector  $\epsilon_k$  is deliberately introduced in  $\mathbf{W}_k$ . Let  $\tilde{\mathbf{W}}_k = \mathbf{W}_k - \epsilon_k$  be the perturbed weight vector. The LMS error signal at time  $k$  is given by

$$\tilde{e}_k = d_k - \mathbf{X}_k^T \tilde{\mathbf{W}}_k = d_k - \mathbf{X}_k^T \mathbf{W}_k + \mathbf{X}_k^T \epsilon_k. \quad (8)$$

Assuming that the learning rate  $\mu$  is equal to  $1/2$ , the weight vector at time  $k+1$  is given by

$$\begin{aligned} \tilde{\mathbf{W}}_{k+1} &= \tilde{\mathbf{W}}_k + \tilde{e}_k \bar{\mathbf{X}}_k \\ &= \mathbf{W}_{k+1} - (\mathbf{I} - \bar{\mathbf{X}}_k \mathbf{X}_k^T) \epsilon_k, \end{aligned} \quad (9)$$

where  $\mathbf{I}$  is the  $N \times N$  identity matrix. Similarly, the weight vector can be evaluated at times  $k+2, k+3, \dots$  and in general, for any time  $k+j$ , one has<sup>1</sup>

$$\tilde{\mathbf{W}}_{k+j} = \mathbf{W}_{k+j} - \prod_{m=0}^{j-1} (\mathbf{I} - \bar{\mathbf{X}}_{k+m} \mathbf{X}_{k+m}^T) \epsilon_k. \quad (10)$$

<sup>1</sup> It can be verified that the order in which the matrix multiplies are effected is irrelevant. This justifies the otherwise ambiguous notation  $\prod_m$ .

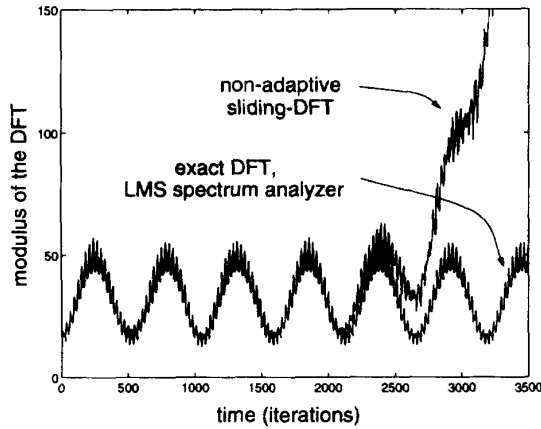


Fig. 2. Recursive implementations of the DFT with limited precision.

Without loss of generality, it can be assumed that  $k = N$  so that

$$\begin{aligned} \tilde{\mathbf{W}}_{N+j} &= \mathbf{W}_{N+j} - \prod_{m=0}^{j-1} (\mathbf{I} - \mathbf{R}_{N+m}) \epsilon_N \\ &= \mathbf{W}_{N+j} - \prod_{m=0}^{j-1} (\mathbf{I} - \mathbf{R}_m) \epsilon_N, \end{aligned} \quad (11)$$

where  $\mathbf{R}_m \triangleq \mathbf{I} - \bar{\mathbf{X}}_m \mathbf{X}_m^T$ .

As seen previously, the vectors  $\{\mathbf{X}_0, \mathbf{X}_1, \dots, \mathbf{X}_{N-1}\}$  form an orthonormal basis in the  $N$ -dimensional space. Similarly, the vectors  $\{\bar{\mathbf{X}}_0, \bar{\mathbf{X}}_1, \dots, \bar{\mathbf{X}}_{N-1}\}$  form another orthonormal basis in the same space. Any error vector  $\epsilon_N$  can be decomposed into its  $N$  components in this last basis:

$$\epsilon_N = \sum_{n=0}^{N-1} \epsilon_N(n) \bar{\mathbf{X}}_n. \quad (12)$$

The product  $\mathbf{R}_m \epsilon_N$  can then be evaluated as

$$\begin{aligned} \mathbf{R}_m \epsilon_N &= (\mathbf{I} - \bar{\mathbf{X}}_m \mathbf{X}_m^T) \epsilon_N \\ &= (\mathbf{I} - \bar{\mathbf{X}}_m \mathbf{X}_m^T) \sum_{n=0}^{N-1} \epsilon_N(n) \bar{\mathbf{X}}_n \\ &= \epsilon_N - \epsilon_N(m) \bar{\mathbf{X}}_m. \end{aligned} \quad (13)$$

The multiplication of the error by the matrix  $\mathbf{R}_m$  eliminates its  $m$ th component and leaves the other components unchanged. Multiplying the residual error vector by  $\mathbf{R}_{m+1}$  will cancel out its  $(m+1)$ th component, and so on. As iterations proceed, the modulus of the error vector decreases monotonically. After  $N$  iterations, all its components have been canceled, and the error reduces to zero.

For illustrative purposes, consider the signal  $x(k) = \sin(2\pi f_1 k/N) + \sin(2\pi f_2 k/N)$  and its 32-point DFT. We wrote a C program implementing the nonadaptive sliding-DFT and the LMS spectrum analyzer algorithms. To demonstrate the effect of limited precision, we rounded off to 7 b the mantissas of the floating point results of all arithmetical operations.<sup>2</sup> For comparison, we also coded the exact DFT of  $x(k)$ . Fig. 2 represents the sum of

<sup>2</sup>In the IEEE standard for floating point arithmetic, the mantissa occupies 23 b, the fraction 8, and the sign one).

the square modulus of the DFT components,  $\sum_{i=0}^{31} |DFT_k(i)|^2$ , as a function of time, for  $f_1 = 0.03$  and  $f_2 = 1.1$ . The DFT given by the LMS spectrum analyzer practically coincides with the exact DFT. The nonrecursive sliding-DFT follows the exact DFT for a while but it eventually diverges.

## V. CONCLUSION

While the nonadaptive sliding-DFT allows roundoff errors to accumulate over time, the LMS spectrum analyzer uses its adaptation loop to automatically eliminate errors in a number of iterations equal to the length of the DFT. It does not require significantly more operations per iteration than the nonadaptive sliding-DFT. These results naturally extend to other transforms once implemented adaptively (see [5] for a generalization of the LMS spectrum analyzer to other orthonormal transforms). For these reasons, we recommend the use of the LMS spectrum analyzer for any application where a sliding orthonormal transform must be performed over long trains of data.

## REFERENCES

- [1] L. R. Rabiner and B. Gold, *Theory and Application of Digital Signal Processing*. Englewood Cliffs, NJ: Prentice-Hall, 1975.
- [2] B. Widrow, Ph. Baudrenghien, M. Vetterli, and P. F. Titchener, "Fundamental relations between the LMS algorithm and the DFT," *IEEE Trans. Circuits Syst.*, vol. CAS-34, no. 7, pp. 814-819, July 1987.
- [3] B. Widrow, J. M. McCool, and M. Ball, "The complex LMS algorithm," *Proc. IEEE*, vol. 63, pp. 719-720, Apr. 1975.
- [4] S. S. Narayan, A. M. Peterson, and M. J. Narasimha, "Transform domain LMS algorithm," *IEEE Trans. Acoustics, Speech, Signal Process.*, vol. ASSP-31, no. 3, pp. 609-615, June 1983.
- [5] S.-S. Wang, "LMS algorithm and discrete orthogonal transforms," *IEEE Trans. Circuits Syst.*, vol. 38, no. 8, pp. 949-951, Aug. 1991.

## A Class of Second-Order Integrators and Low-Pass Differentiators

Mohamad Adnan Al-Alaoui

**Abstract**—A novel class of stable, minimum phase, second-order, low-pass IIR digital differentiators is developed. It is obtained by inverting the transfer functions of a class of second-order integrators, stabilizing the resulting transfer functions, and compensating their magnitudes. The class of second-order integrators is obtained by interpolating the traditional Simpson and trapezoidal integrators. The resulting integrators have a perfect  $-90^\circ$  phase over the Nyquist interval and could better approximate the ideal magnitude response than either of the two traditional integrators. In addition to the above two integrators, the Tick integrator is also a member of the class. The resulting integrators and differentiators extend the frequency range of operation beyond that possible by using either of the two traditional integrators. The low order and high accuracy of the filters make them attractive for real time applications.

## I. INTRODUCTION

The basic concept came from observing that the ideal integrator response lies between the responses of the traditional trapezoidal and

Manuscript received January 20, 1994; revised November 24, 1994. This work was supported in part by the Research Board of the American University of Beirut, Beirut, Lebanon. This paper was recommended by Associate Editor I. Pitas.

The author is with the Electrical and Computer Engineering Department, The American University of Beirut, Beirut, Lebanon.

IEEE Log Number 9410007.